

The SLIM Spectrometer

Kevin M. Cantrell[†] and James D. Ingle, Jr.^{*}

Department of Chemistry, Oregon State University, 153 Gilbert Hall, Corvallis, Oregon 97331-4001

A new spectrometer, here denoted the SLIM (simple, low-power, inexpensive, microcontroller-based) spectrometer, was developed that exploits the small size and low cost of solid-state electronic devices. In this device, light-emitting diodes (LED), single-chip integrated circuit photodetectors, embedded microcontrollers, and batteries replace traditional optoelectronic components, computers, and power supplies. This approach results in complete customizable spectrometers that are considerably less expensive and smaller than traditional instrumentation. The performance of the SLIM spectrometer, configured with a flow cell, was evaluated and compared to that of a commercial spectrophotometer. Thionine was the analyte, and the detection limit was $\sim 0.2 \mu\text{M}$ with a 1.5-mm-path length flow cell. Nonlinearity due to the broad emission profile of the LED light sources is discussed.

Small portable spectrophotometers are useful in field applications and process monitoring. Several companies such as Hach and Chemetrics sell battery-powered, filter-based instruments that are generally used with reagent kits tailored to a specific determination. Often in the design of these spectrometers compromises are made in the selection of the optoelectronic components to allow for reduced size and cost.

Several researchers have used light-emitting diode (LED) light sources to replace traditional spectrophotometric sources in which the small size, exceptional stability, low cost, low power consumption, and robust nature of these LEDs allow for the design of new spectrometers. Dasgupta and co-workers provided an excellent review article of the spectrometric applications of LEDs,¹ demonstrated the use of multiple LED-based spectrometers to correct errors due to refractive index and turbidity in FIA,² and designed several novel flow cells around LED light sources.³

Hauser^{4,5} focused on using several LEDs to gain the functionality of a multiple-wavelength spectrometer. Because LED emission profiles are somewhat narrower (20–40 nm) than typical molecular bands (50–100 nm), a device that incorporates multiple LEDs can function as a multiple-wavelength spectrometer that covers a

large portion of the visible band. Commercially available multi-emitter LEDs (two- and three-color varieties), as well as individual LEDs coupled together with fiber-optic hardware, have been investigated. Huang et al.⁶ also explored the applications of multiple-emitter LEDs and has used rapid microcomputer-controlled modulation to produce a FIA detector with low drift. Worsfold and Clinch^{7–9} focused on the applications of LED-based spectrometers coupled with simple FIA techniques in the areas of environmental monitoring and process control. These rugged spectrometers were used to determine water quality parameters such as phosphate, nitrate, and ammonia and were able to collect data unattended for periods of approximately one week.

In this work, we outline the design and construction of a new type of reconfigurable miniature spectrometer based on modern semiconductor technology that incorporates an array of useful features. The design philosophy de-emphasizes the complexity, optical sophistication, computational ability, accuracy, resolution, and processing power usually found in benchtop spectrometers. Instead, characteristics such as miniaturization, automation, reduced cost, low power consumption, simplicity, and reconfigurability are emphasized. Spectrometers of this design have uses in the areas of flow stream/process monitoring, field sampling, environmental monitoring, and disposable applications. This design is intended as a complete basic spectroscopic platform that can be tailored to a specific analytical determination. This device incorporates a LED light source, photodetector (photodiode based), flow cell, battery, reprogrammable microprocessor, clock, memory for data-logging capability, and both a computer and a user interface on a single circuit board with the footprint of a credit card. The spectrometer is intended to be inexpensive, small, rugged, and versatile.

The spectrometer was evaluated in a flow cell configuration with thionine as the analyte. Calibration and noise data were obtained and compared to results obtained with a commercial spectrometer under equivalent conditions. The effect of the broad emission of the red, yellow, and blue LEDs on the calibration curves is discussed.

INSTRUMENTATION

General Considerations. The new spectrometer, denoted the SLIM (simple, low-power, inexpensive, microcontroller-based) spectrometer, is similar to traditional spectrophotometers in many respects. Table 1 shows a comparison of the common functional

* Corresponding author: (phone) 541-737-6743; (e-mail) James.Ingle@orst.edu.

[†] Present address: Department of Chemistry, University of Portland, Portland, OR 97203.

(1) Dasgupta, P. K.; Bellamy, H. S.; Liu, H.; Lopez, J. L.; Loree, E. L.; Morris, K.; Petersen, K.; Mir, K. A. *Talanta* 1993, 40, 53–74.

(2) Liu, Hanghui; Dasgupta, P. K. *Anal. Chim. Acta* 1994, 289, 347–353.

(3) Jambunathan, Sivakumar; Dasgupta, P. K.; Wolcott, D. K.; Marshall, G. D.; Olson, D. C. *Talanta* 1999, 50, 481–490.

(4) Hauser, P. C.; Rupasinghe, T. W. T.; Cates, N. E. *Talanta* 1995, 42, 605–612.

(5) Hauser, P. C.; Rupasinghe, T. W. T.; Tan, R. *Chimia* 1995, 49, 492–494.

(6) Huang, J.; Liu, H.; Tan, A.; Xu, J.; Zhao, X. *Talanta* 1992, 39, 589–592.

(7) Worsfold, P. J.; Clinch, J. R. *Anal. Chim. Acta* 1987, 197, 43–50.

(8) Clinch, J. R.; Worsfold, P. J. *Anal. Chim. Acta* 1987, 200, 523–531.

(9) Clinch, J. R.; Worsfold, P. J. *Anal. Chim. Acta* 1988, 214, 401–407.

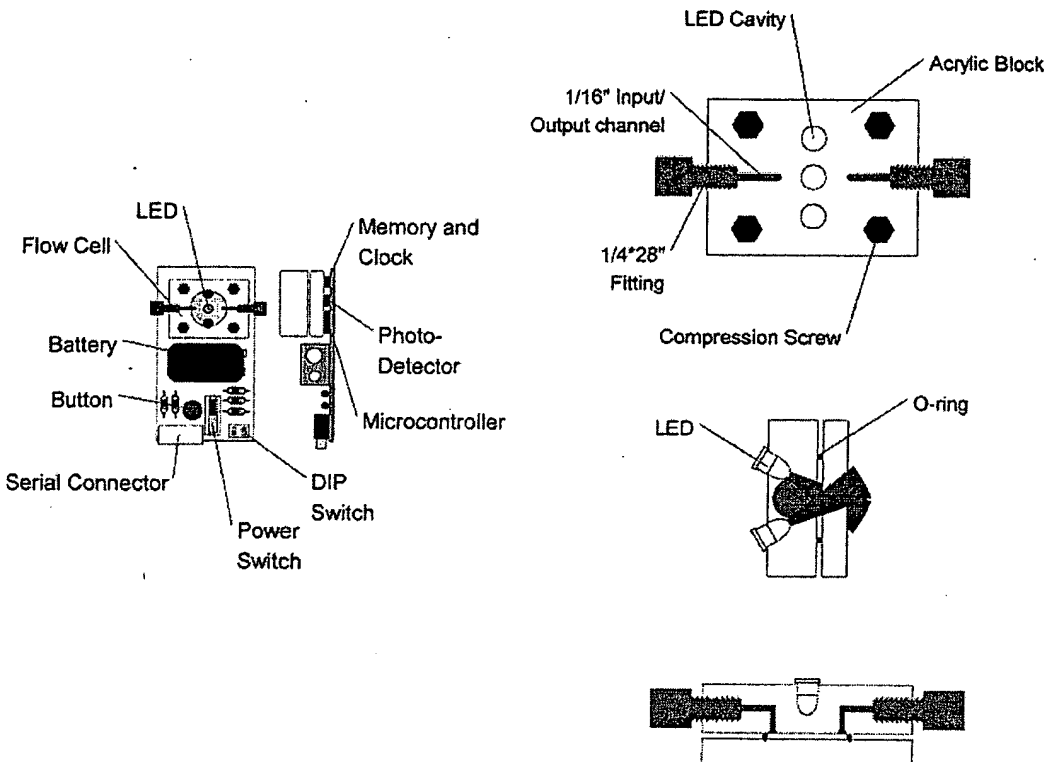


Figure 1. Instrumental diagram indicating the layout of the basic components of the solid-state spectrometer. These components include the LED light source, photodetector, microcontroller, clock, memory, battery, serial connector, and switches. The circuit board dimensions are 2 in. by 4 in. by 1.5 in. The outside dimensions of the flow cell are 2 in. wide, 1 in. long, and $\frac{3}{4}$ in. deep. The cones in the middle figure indicate the 30° beams emitted by the two LEDs.

Table 1. Elements of Conventional and SLIM Spectrometers

component	conventional	SLIM
light source	tungsten lamp	LED
sample delivery	cuvette	acrylic flow cell
detector	photodiode, PMT, or diode array	photodiode IC
data storage	computer disk	EEPROM
control unit	PC	microcontroller

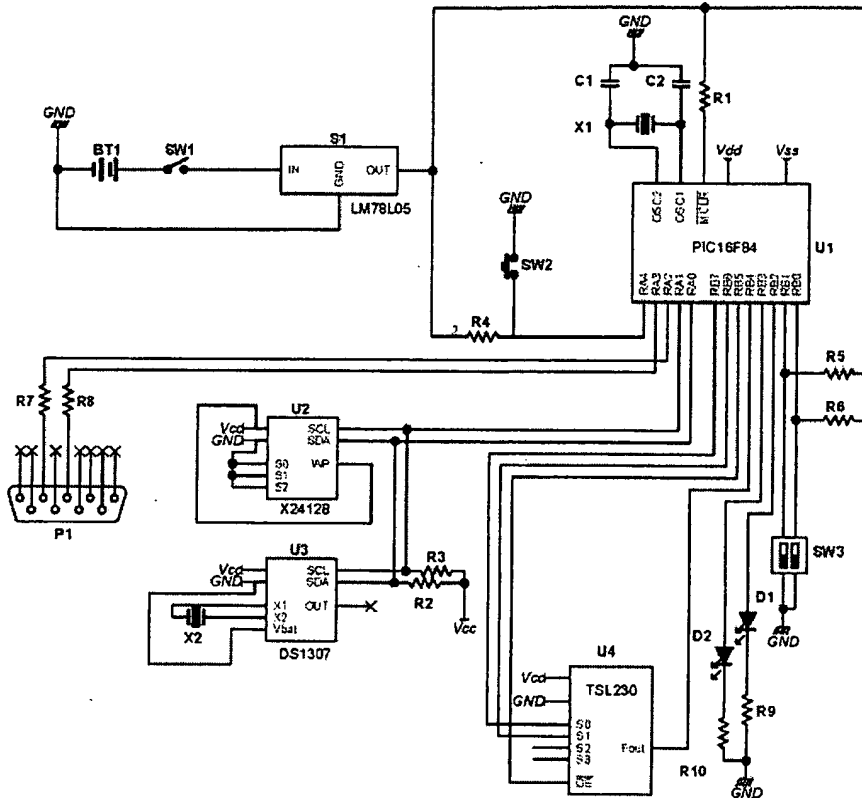
elements of a spectrometric system. The new device was developed with environmental monitoring in mind, and many of the incorporated features relate to this type of measurement. For example, it is capable of operating in an unattended data-logging mode in which the user selects a sampling interval and allows the unit to collect data. The user then returns and downloads the logged data into a laptop computer for processing and interpretation. These devices do not contain a built-in mechanism for display and rely on a PC or supplementary electronics for this function.

The basic function of this device is that of a spectrometer, to measure the intensity of light passing through a sample. To achieve this function, a programmed microcontroller turns on a LED light source and measures intensity as the frequency output from a photodetector chip (a radiant power-to-frequency converter). The spectrometer then stores this information and continues to collect data over time.

The diagram in Figure 1 outlines the functional elements of the spectrometer and illustrates the design for the flow cell. This cell was designed to accommodate a reagent, such as an indicator dye, that is immobilized on a transparent film but also accommodates solutions. In previous and ongoing work immobilized redox indicators have been used for monitoring the redox status of anaerobic systems.^{10,11} For this type of application, the cell must be demountable and accommodate a replaceable disk of immobilized reagent (~2 cm in diameter). The sample solution is contained in a space defined by an O-ring compressed by two sheets of acrylic (~500- μ L internal volume). The thicker of these sheets is machined with tapped holes to accept $\frac{1}{4}$ -in. 28 male fittings for connecting to tubing. The sample solution is directed into and away from the sample cavity by right-angle drilled holes. The thick side of the cell body also contains holes drilled to accommodate three LED light sources. The LED cavity in the center of the cell is pointed directly at the other side. LED cavities adjacent to the center of the cell are oriented a 30° angle so that light from the inserted LEDs illuminates the same photodetector in the center of the opposite side of the cell. The screws that compress the O-ring between the sides of the cell also affix the entire flow cell to a circuit board where the photodetector chip is soldered in the proper position. The path length of the cell varies with the degree of O-ring compression. This variation is not critical

(10) Lemmon, T. L.; Westall, J. C.; Ingle, J. D. Jr. *Anal. Chem.* 1996, 68, 947–953.

(11) Jones, B. D.; Ingle, J. D., Jr. *Talanta* 2001, 55, 699–714.



Reference:	Value:	Description:
U1	PIC16F84	Microcontroller
U2	X24128	Serial EEPROM
U3	DS1307	Real Time Clock
U4	TSL230	Light to Frequency Converter
S1	LM78L05	Voltage Regulator
SW1	SWITCH	Sliding Power Switch
SW2	BUTTON	Momentary Pushbutton
SW3	SWITCH	2x DIP Switch
X1	4 MHz	Crystal Oscillator
X2	32 kHz	Crystal for RTC
P1	DB9 FEMALE	Serial Connector
BT1	9 V	Battery
C1,C2	22 pF	Decoupling Capacitor
D1,D2	LED	See Text
R1,R2,R3,R4,R5,R6	4.7 kΩ	Pull Up Resistor
R7	1 kΩ	Resistor
R8	22 kΩ	Resistor
R9, R10	330 Ω	Resistor

Figure 2. Schematic of the SLIM spectrometer.

when immobilized indicators are used, but spacers would be necessary for exact control of the path length for solution work in which the path length must be known. In this work, the path length was ~ 1.5 mm. The flow cell mounts via the four holes and occupies the upper one-third of the circuit board.

Electronic Components. The electronic components were selected to match the low cost and low power consumption of

the light-emitting diodes. The total cost of the integrated circuits and LEDs used to construct the spectrometer is about \$25. A sample schematic is provided in Figure 2. The life of the battery is determined by the duty cycle of the LEDs. An alkaline 9-V battery can power an LED with 10 mA of current for ~ 60 h of continuous operation. If the data are acquired once per minute, this battery should power the instrument for two months.

The IC selected to serve as the embedded microcontroller in these devices is the PIC16F84 (Microchip Technologies Inc.). This chip is an 8-bit MCU (microcontroller) with 1K of program memory and 68 bytes of data RAM. It is a member of their flash family of products, so it can be electrically erased, allowing for rapid prototyping and code development. It is a reduced instruction set computer (RISC) paradigm chip so there are only 35 assembly language instructions. The MCU has 13 I/O lines, and each line can source 20 mA or sink 25 mA of current. In this application a 4-MHz crystal was used as the oscillator. The MCU chip internally divides the resonant frequency of this crystal by four to derive an instruction clock rate of 1 MHz. An 8-bit MCU was selected because its cost, size, power consumption, and computational power are well matched to this particular application. This model and manufacturer was selected because the cost of programming hardware and software were minimal, and the company provides extensive literature and programming examples for smaller scale operations.

The program for the microcontroller was written in a high-level BASIC programming language and compiled into assembly instruction with the PIC Basic Pro compiler (MicroEngineering Labs Inc.). This high-level programming language makes complex activities such as communicating with other ICs much easier to code.

LEDs from a variety of manufacturers were evaluated. For this work a red and a yellow-orange LED from Jameco and a blue LED from Nichia were used as the light sources for the spectrometer. The LEDs are driven by a battery with a simple current-limiting resistor.

The photodetector was the TSL230 programmable light-to-frequency converter manufactured by Texas Instruments. Although TI no longer manufactures this part, Texas Advanced Optoelectronic Solutions (TAOS) has been granted a license to produce and market their family of optoelectronic sensors. This chip integrates a configurable grid of photodiodes and a current-to-frequency converter in a single package. With no additional electronic components, it provides a TTL square wave with a frequency proportional to light intensity. This photodiode's sensitivity is adjustable over 3 orders of magnitude by manipulating two input lines to change the active readout area of the photodetector. The output frequency can be divided by 1, 2, 10, or 100. Division by 2 or more is necessary to produce a 50% duty cycle. This photodetector is ideal for this application because no separate ADC chip or domain converters are required.

A DS1307 serial real time clock (Dallas Semiconductor) was used as the timekeeping device. This IC uses a 38.768-kHz crystal to keep track of seconds, minutes, hours, day, date, month, and year. It communicates as a slave on the I²C bus developed by Phillips.¹² This communication protocol is a two-wire synchronous serial bus that supports multiple devices connected to the same bus.

An X24128 128K-bit serial EEPROM (Xicor) serves as the memory for this device. This memory is organized in a 16K x 8-bit fashion. It is used to store the time stamp information along with light intensity information in a formatted data block. Both read and write operations are controlled via the same I²C bus used

(12) Phillips Semiconductor. <http://wwwus.semiconductors.philips.com/acrobat/varioust/I2sbus.pdf>, 1995.

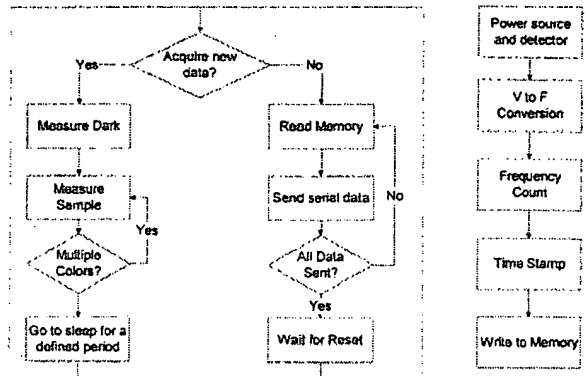


Figure 3. Flow diagram of the steps in the MCU program. The decision point "Acquire new data?" is determined by the state of the pushbutton switch. The sequence of events on the right is executed each time the spectrometer measures an intensity.

for communication with the real time clock. This component was selected because it provides a functional amount of storage with a minimum of hardware lines and software overhead for nonvolatile data storage and retrieval. With this EEPROM, the spectrometer can hold over 1000 data acquisitions. The four intensity readings require two bytes of storage each, and the time stamp requires four bytes. If data are acquired once per minute, the memory will suffice for approximately 1 day, or if the data are acquired every hour, the memory can store approximately 2 months of data. The memory can be easily expanded by adding more EEPROM chips (currently up to a factor of 8). The storage capacity of these ICs is constantly being increased, and storage space is not anticipated to be an issue in the future.

Operation. The device is built around a simple user interface involving a single button and a power switch. The software flowchart in Figure 3 identifies some of the basic steps performed during operation. Pressing the button instructs the device to collect data. When the power switch is turned on and the button is not pressed, the device sends out all of the data that it has stored in the EEPROM over its serial port. If the button is then pressed (after the download of the data), the device begins acquiring new data and appends these new data points to those already stored in memory. If the button is pressed when the power switch is initially turned on (before the download of the existing data), then the old data are discarded and the new data are stored starting from the base memory address.

Any time the power is switched on the real time clock is reset to zero. The time stamp is simply the number of days, hours, minutes, and seconds that have elapsed since the power was switched on. If the device is used in the append mode, the data will contain multiple time zero stamps. The operator must keep track of the times when the device was turned on so that a correspondence between the time stamp and actual time can be established.

Most of the important variables for signal acquisition such as the sensitivity of the photodiode, integration time, and number of sample points to average are set when the device is programmed. Changing these variables requires that the user change them in the microcontroller's program, recompile the program with the new variables, remove the microcontroller, reprogram

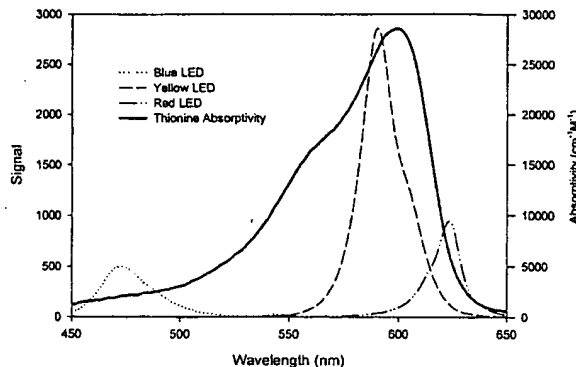


Figure 4. Profiles of the emission of the LEDs and of thionine absorptivity. The LED emission profiles were obtained with a CCD-type spectrometer and are not corrected for the grating efficiency or the detector responsivity. All LEDs were $T\ 1\frac{3}{4}$ (5-mm) size. The blue LED (λ_{max} at 473 nm) was operated with a 22-k Ω resistor at ~ 0.2 mA of current. The yellow LED (λ_{max} at 590 nm) was operated with a 470- Ω resistor at ~ 10 mA of current. The red LED (λ_{max} at 623 nm) was operated with a 2.2-k Ω resistor at ~ 2 mA of current.

the flash memory of the chip, and return the chip to the device. This process requires some expertise, knowledge of the structure of the program, and understanding of the programming hardware. Although it is somewhat inconvenient, most of the variables are rarely changed for a given application, and their inclusion in the program greatly simplifies the user interface.

One parameter that may change is the sampling interval (the time between sampling events). To facilitate this customization of the device, a set of two DIP switches, each with two states, provides four possible settings. In the current version of the spectrometer, settings 1 and 2 designate a fixed sampling interval: one short and one long (e.g., 1 and 60 s). With setting 3, the instrument uses the last value it was sent via its serial connection as the sampling interval. It stores this sampling interval in a fixed location in the EEPROM memory. Setting 4 places the device under direct control via the serial connection. The PC (or other device) to which it is connected may send it a new sampling interval (which would be subsequently used if the switch were set to the third position), or it may initiate a sample event immediately. In this manner, the device can operate as a tethered spectrometer with data acquisition and display managed by a spreadsheet or stand alone program running on a PC.

EXPERIMENTAL SECTION

The performance of the cell and spectrometer was characterized with simple colored solutions rather than films with different concentrations of an immobilized reagent because it is easier to prepare a series of solutions with known concentrations. The redox indicator dye thionine was selected as the analyte since it is of interest in other redox monitoring applications.^{10,11} Figure 4 shows the relationship between the emission profiles of the LEDs selected as light sources and the absorption profile of thionine.

The absorbance of the flowing colored solution was measured simultaneously with a HP diode array spectrometer (Hewlett-Packard 8452A) and the SLIM spectrometer. The HP spectrometer serves as a reference for benchmarking the SLIM spectrometer. A peristaltic pump (Alitea) was used to circulate the solution

through a closed loop consisting of a 250-mL reservoir, an in-house flow cell (3-mm path length) positioned in the HP spectrometer, and the flow cell of the SLIM spectrometer. The flow rate was ~ 2.5 mL/min.

At the beginning of the experiment, the reservoir was filled with 150 mL of deionized water from a Millipore ion exchange system and continually stirred with a magnetic stir bar. This water was circulated for ~ 5 min, and trapped gas bubbles were removed from both flow cells. A reference spectrum was then collected and stored on the HP spectrometer, and all subsequent values measured by this instrument were stored as absorbance. The HP instrument was configured in kinetics mode and set to monitor four wavelengths (400, 552, 600, and 700 nm) at a 10-s interval.

Because the SLIM spectrometer is not configured to calculate absorbance, the data were stored as signals proportional to transmitted intensities. The embedded controller simply counts the pulses output by the photodetector chip for a defined period of time. This quantity is linearly related to light intensity. From the final data set described later, a spreadsheet was used to calculate absorbance (A) from eq 1. The average of the first five

$$A = -\log \left[\frac{(\text{sample intensity} - \text{dark intensity})}{(\text{blank intensity} - \text{dark intensity})} \right] \quad (1)$$

signal values with each LED was used as the blank intensity in all absorbance calculations.

The SLIM spectrometer was configured in the data-logging mode and set to monitor the transmitted intensities (counts from the photodetector) of three LEDs (blue, yellow, and red) and the dark signal (all LEDs off). The current-limiting resistor for each LED was adjusted until the responses with each lamp were similar. The photodetector sensitivity was adjusted to the maximum (area) with division of the output frequency by 2. With a 100-ms integration time, the dark signal was measured first, followed by the signals of the three LEDs in succession. This cycle was repeated 10 times until each quantity was measured for 1 s and the total measurement time was 4 s. This period was followed by a 10-s (adjustable via the DIP switches) sleep time in which the instrument enters a low-power consumption mode. The modulation during data acquisition of the sources provides some suppression of 60-cycle noise and other nonfundamental shifts or drift in the background ambient light level. The spectrometer was also wrapped in black felt to further reduce the noise associated with fluctuations in room light.

Both spectrometers were activated simultaneously so that they marked the same initial time. Once the experiment was underway, 100–250- μ L aliquots of 2 mM thionine were added to the reservoir at ~ 2.5 -min intervals. The aliquots were added with an Eppendorf pipet to a continuously stirred reservoir. No effort was made to be precise about the concentration of the solutions because absorbance was continually measured by the HP spectrometer. This incremental addition of colored compound allowed for 40 distinct concentrations of analyte to be measured several times each by both spectrometers in an experiment with a 100-min duration. The absorbance at the absorption band maximum (as measured by the HP spectrometer) ranged from 0 to 2 AU over the course of the experiment as the thionine concentration increased from 0 to ~ 300 μ M. At the end of the experiment, the

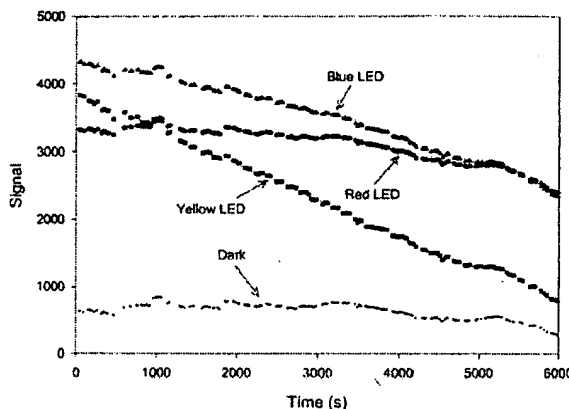


Figure 5. Time dependence of the uncorrected photodetector signals measured with the SLIM spectrometer. The "drift" in the dark signal level and low-frequency fluctuations in all signals are "drifts" in the background (ambient light) signal because the flow cell was not light-tight.

data stored in each instrument were saved to a computer disk and imported into a spreadsheet.

RESULTS AND DISCUSSION

Figure 5 shows time dependence of the measured photodetector signals with the three LEDs and the dark signal as the absorbance increased due to the periodic addition of thionine. Because it takes time to completely flush the flow path and sample cells and achieve a uniform composition throughout the system, the concentration of the analyte had not stabilized during data acquisition immediately following the addition of thionine. The derivative of the dark-corrected signal with respect to time was used as a criterion to eliminate data points in which the signal was dramatically different from the previous signal. Because fewer measurements were taken with the SLIM spectrometer and a one-to-one correspondence was desirable, only the data points from the HP spectrometer that matched up closely (5 s or less) in time with the SLIM spectrometer were included in the final data set. In summary, data points taken at times when the concentration of analyte was changing or when the HP acquisition time did not match the SLIM acquisition time were removed. After the removal of these points, ~250 data points remained. From these remaining values, the absorbances were then calculated with eq 1.

Figure 6 shows the calibration curves based on the absorbances measured with the HP spectrometer (3-mm path length) at two wavelengths and with the SLIM spectrometer (1.5-mm path length) with three different LEDs. The absorbance at 552 nm (about half that at the band maximum at 600 nm) measured with the HP spectrophotometer was used to estimate the thionine concentration in the flow cells at a given time. Because the absorbance at the band maximum (600 nm) exhibits nonlinearity at higher absorbances, it was not used to define the concentration axis. The absorptivity at 552 nm was determined from the absorbance previously measured at 552 nm with the HP spectrometer, a 1-cm-path length cuvette, and a 20 μM solution. A separate calibration curve obtained for thionine standard solutions at 552 nm in a standard 1-cm sample cell exhibited good linearity up to an absorbance of 1 or more. The calibration curve based on

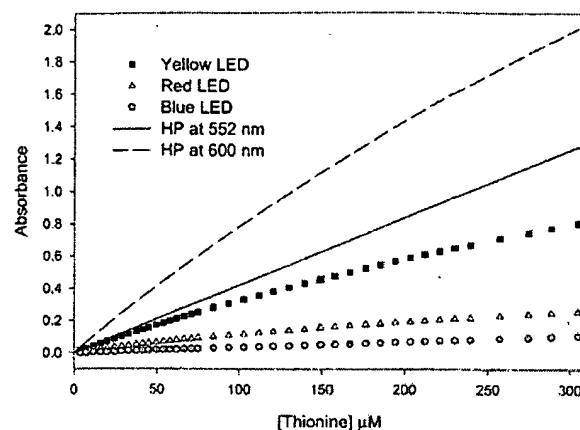


Figure 6. Calibration curves with the HP spectrometer monitoring different wavelengths and with the SLIM spectrometer with different LED light sources. The initial calibration slopes are as follows: HP at 600 nm, 0.0089 AU/ μM ; HP at 552 nm, 0.0042 AU/ μM ; yellow LED, 0.0036 AU/ μM ; red LED, 0.0016 AU/ μM ; blue LED, 0.0003 AU/ μM . The path length of the SLIM spectrometer is half that of the HP spectrometer.

the data from the HP spectrometer at 552 nm is linear because this wavelength was used to define the concentration axis. Due to the difference in path length, the polychromatic nature of the LEDs, and their often nonoptimal overlap with the absorption band of thionine (Figure 3), the initial slopes observed for the calibration curves are a factor of 2–20 smaller than the slope of the calibration curve for the HP spectrometer obtained at the band maximum. The initial slopes with the HP spectrometer (600 nm) and the SLIM spectrometer with the yellow LED light source are very similar if the path lengths are normalized.

The nonlinearity for all conditions (except 552 nm) is apparent at concentrations above $\sim 50 \mu\text{M}$. Note that the curve derived from the HP spectrometer at the band maximum (600 nm) shows a significant deviation from linearity. Because the LEDs used in the SLIM spectrometer emit over a fairly broad wavelength region (the width at half-height is $\sim 25 \text{ nm}$), deviations from linearity due to polychromatic radiation are expected. This nonlinearity is a direct result of the nature of the shape of the absorbance profile within the envelope described by the LED's emission. Those LEDs that emit over a wavelength region where the absorptivity changes dramatically (red and yellow) give rise to more extreme deviations from linearity than the LED that emits in a region where the absorptivity is relatively constant (blue).

To model these nonlinear calibration curves, eq 2 was employed, where E_λ is the "emission-response profile" of an LED

$$A_{\text{predicted}} = -\log \sum_{\lambda} 10^{(\epsilon_{\lambda} b)} E_{\lambda} / \sum_{\lambda} E_{\lambda} \quad (2)$$

and ϵ_{λ} is the molar absorptivity profile of the absorbing species. The emission-response profile and molar absorptivity profile were determined with a CCD spectrometer (Ocean Optics) from 400 to 800 nm with each data point per pixel corresponding to approximately a 0.3-nm range. The emission-response profiles of the LEDs were corrected for differences in the responsivity of

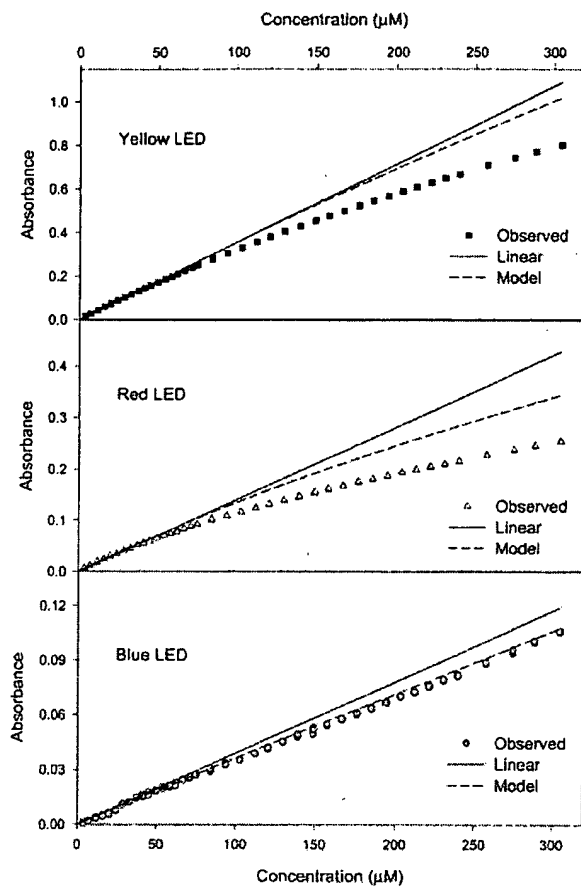


Figure 7. Comparison of predicted, linear, and observed calibration curves with the SLIM spectrometer. The predicted curves (model) are based on eq 2. The linear curves are based on extrapolation of the linear portion of the curves at low concentrations (0–25 μM for the yellow and red LED data, 0–50 μM for the blue LED data).

the photodiode and CCD detectors and the grating efficiency of the dispersive instrument. Because these corrections are approximations based on available data and do not include corrections for optical coatings, the true emission-response profile of the LED is somewhat different from that assumed for the calculation in eq 2.

These calculations were performed for the blue, red, and yellow LEDs used in this spectrometer, and results are given in Figure 7. For the yellow and red LEDs, the experimental deviation from linearity is significantly greater than the theoretical deviation from linearity predicted by this model. These differences are attributed to incorrect values of E_k used in eq 2, stray light, and possible nonlinearity due to chemical effects. The closest match with the calculated values is observed with the blue LED, where the absorptivity of thionine is lowest and relatively flat over the emission profile. The model correctly predicts that the degree of deviation from linearity at low concentrations occurs in the order red, yellow, and blue LED source. Although this model is useful in understanding the performance of the spectrometer, its primary value is in the selection of a set of LEDs for a given application. Given a molar absorptivity profile of an analyte and the emission-response profiles of several LEDs, this model can be used to

Table 2. Comparison of the Precision of Commercial and SLIM Spectrometers^a

source or wavelength	pooled standard deviation (mAU)
yellow LED	0.68
red LED	0.46
blue LED	0.47
HP at 400 nm	0.18
HP at 552 nm	0.33
HP at 600 nm	0.42
HP at 700 nm	0.24

^a These standard deviations are pooled together according to eq 3, where N is the number of determinations in a group and s is the standard deviation of the group: $s_{\text{pooled}} = (\sum_a (N_a - 1) s_a^2 / \sum_a N_a - d)^{1/2}$ (3).

compare the predicted sensitivities and linear ranges of spectrometers configured with various LED light sources.

The absorbances calculated for a given LED were regressed against concentrations to give a calibration equation that relates the response of the instrument to concentration. Both a first-order fit (without an intercept) and a second-order fit (without an intercept) were performed with the absorbance data from the three LEDs used in this experiment, and the standard calibration errors of the concentration estimates were compared. This figure of merit indicates the agreement between the values predicted by substituting the SLIM spectrometer data into the respective calibration equations and the true concentration of thionine. The second-order fit provides ~1 order of magnitude reduction in the standard error compared to the first-order fit for measurements over a large range of concentrations. Note that useful calibration information can even be obtained with a very poor match between the LED emission and analyte absorption. For example, in this application the yellow or red LED sources provide a second-order calibration curve with a standard error of less than 1 μM thionine in a cell with only a 1.5-mm path length.

The precision of the absorbance measurement of the LED-based spectrometer was compared to the precision of the HP diode array spectrometer for this simple system. Twenty concentrations were measured multiple times (4–19), and the standard deviations of the measured absorbances were calculated. Significant differences in the standard deviation for different absorbances were not observed. The pooled standard deviations obtained with both spectrometers are summarized in Table 2. In this application, the blank noise of the SLIM spectrometer is comparable to that of a commercial diode array spectrometer. The blank noise is greater than expected with a diode array spectrometer because measurements are made on a flowing stream over a long time period.

To fully characterize the noise characteristics of the SLIM, a much higher number of repetitive measurements would be needed to obtain better estimates of the standard deviation in various signals. However, all experimental experience with the SLIM suggests that 0% T noise or noise in the dark signal from the photodiode and associated circuitry is limiting (i.e., the noise in photosignals is equivalent to the noise in the dark signal). Under the conditions used, this 0% T noise is ~0.1% of a typical reference signal. Flicker noise from the LED or photon shot noise is insignificant. Additional noise can be caused by fluctuations in

ambient light levels if the SLIM is not shielded properly or by bubbles or particles in the flow cell.

The detection limit depends on the ratio of the blank noise to the calibration slope at low concentrations. For this application, the detection limit for thionine with the yellow, red, and blue LEDs in the SLIM spectrometer is estimated to be worse by about a factor of 2, 4, and 13, respectively, relative to the $0.12 \mu\text{M}$ detection limit with the HP spectrometer at the absorbance maximum of 600 nm (based on twice the pooled standard deviation of the signal at several concentrations divided by the initial calibration slope). This loss in detectability is a result of the lower calibration curve slope realized with the LED light sources emitting over a broad range of analyte absorptivities. It is possible to place an absorption or interference filter with an appropriately small diameter in front of the LED to narrow the emitted wavelength range and thus increase the calibration slope and improve the detection limit.

In the design of the SLIM spectrometer, selectivity, detection limit (calibration slope), and linearity are somewhat compromised in order to gain simplicity, low cost, small size, low power consumption, remote data-logging capability, and versatility. Its performance is still quite suitable for many applications where the monitored species is a dominant absorbing species in the sample with a concentration well above the typical detection limit. The SLIM spectrometer is sufficiently sensitive to accurately measure a 2 mAU change. Although the linear range with LEDs having broad emission profiles is limited, the data are easily calibrated with a second-order equation, and much of the dynamic range is preserved.

CONCLUSIONS

A new class of absorption spectrometer has been described that makes use of modern semiconductor technology. We have demonstrated that this suite of components can produce quantitative information and remain inexpensive, small, and adaptable. The focus of this paper is to outline the fundamental components and characterize their performance for a simple application.

There are several significant differences between the SLIM spectrometer and LED-based spectrometers previously described in the literature. In this new design, the small size, low power consumption, and simplicity of the LED light source is well matched to the other components of the spectrometer. The result is a complete, self-contained, and compact unit about the size of bath soap capable of unattended data collection over a period of months. Due to their polychromatic nature, we have also tried to offer advice for making accurate measurements with LEDs and provide guidance on the nonlinearity associated with these sources. In essence, we are building on the current literature concerning LED light sources and their applications by suggesting a sample compartment, detector, controller, memory, user interface, and calibration strategy necessary to complete the analytical instrument.

The comparison of the SLIM to a commercial spectrometer demonstrates that this device can generate useful results (comparable to a benchtop instrument) even though components were selected for other characteristics. The SLIM cannot duplicate a high-performance spectrometer in terms of wavelength resolution or noise. The SLIM is intended to be used in application where a dominant absorbing species is monitored and baseline noise levels of ~ 1 mAU are sufficient.

The SLIM is not tailored to a specific analytical determination. Instead, we describe a basic set of components that may find application in a variety of analyses. In other more specific applications, the benefits of this approach are more clearly realized. For example, the low power consumption and unattended data storage features of the spectrometer are less critical for benchtop applications.

The versatility of the SLIM platform has been demonstrated in our laboratory where we are emphasizing environmental monitoring. The SLIM has replaced a commercial HP diode array spectrometer used to monitor the redox state of an immobilized redox indicator in the flow loop of a benchtop anaerobic bioreactor. This same basic design has been reconfigured to accept a standard 1-cm-path length cell. In another application under development, both the source and detector are moved to the same side of the sensor to create a reflectance spectrometer capable of measuring the redox status and pH of a sample in a sealed container. The SLIM platform has been adapted to construct a vertical array of spectrometers in a solid housing that can be driven into the ground to provide subsurface depth profile information about redox transformations over a 3-week period.¹³ The SLIM is also capable of controlling a miniature pumping system, and with the proper reagents, a very small flow injection system can be constructed. Work is currently underway to adapt the SLIM spectrometer to a miniature flow injection device for measuring Fe(II) *in situ*. The same spectrometer, reconfigured without a flow cell, will be used in a teaching application where the cost is low enough for many students to have a spectrometer.

As configured, the SLIM allows simultaneous measurement over three different wavelength regions and potentially of three species with appropriate absorption spectra. We have tested many LEDs with peak wavelengths between 370 and 950 nm with good results. The current LEDs could be replaced with multiple-color LEDs to enhance the capability for multi-channel measurements in specific determinations. With proper statistical data analysis, the instrument could be calibrated to measure one analyte or compensate for one interference per LED light source. Our modeling of instrumental response gives an indication of the suitability of the light source by calculating a theoretical calibration curve for a given analyte. Two or more SLIM devices could be used in series to enhance multiple-component analysis or to employ multiple reagents.

For future specific applications or to provide special characteristics, significant modifications or reconfigurations of the design presented here may be necessary. Our initial intention is to avoid any components that would add to the size, cost, or battery drain of the device unless their inclusion is dictated by the application. For longer term operation, the SLIM would be connected to a larger battery or a power supply and a computer (for data storage). In some remote monitoring situations, the reference signal could only be obtained at the beginning or at end of the experiment. For accurate absorbance measurements, long-term drift in the absolute LED intensity could be important. In this case, a constant-current source (such as an LM317 circuit) or a temperature-

(13) Cantrell, K. The Development and Characterization of Miniature Spectrometers for Measuring Redox Status of Environmental Samples. Ph.D. Thesis, Oregon State University, 2001.

compensated precision current source would increase the stability of the source.

Rearrangement of the optical path would allow for the SLIM to be used in modes of operation other than absorbance. For example, a fluorometer could be easily constructed by changing the flow cell design for a compartment with a 90° angle between the LED source and the detector. The same optical arrangement could be used to measure the light scattering (specifically turbidity) of a sample.

ACKNOWLEDGMENT

Partial funding for this research was provided by the Office of Research and Development, U.S. Environmental Protection Agency, under Agreement R-815738, through the Western Region Hazardous Substance Research Center. The content of this publication does not necessarily represent the views of the agency. The authors express their appreciation to Ted Hinke for his input to the design and construction of the machined components.

AC026015S

**This Page is Inserted by IFW Indexing and Scanning
Operations and is not part of the Official Record**

BEST AVAILABLE IMAGES

Defective images within this document are accurate representations of the original documents submitted by the applicant.

Defects in the images include but are not limited to the items checked:

- BLACK BORDERS**
- IMAGE CUT OFF AT TOP, BOTTOM OR SIDES**
- FADED TEXT OR DRAWING**
- BLURRED OR ILLEGIBLE TEXT OR DRAWING**
- SKEWED/SLANTED IMAGES**
- COLOR OR BLACK AND WHITE PHOTOGRAPHS**
- GRAY SCALE DOCUMENTS**
- LINES OR MARKS ON ORIGINAL DOCUMENT**
- REFERENCE(S) OR EXHIBIT(S) SUBMITTED ARE POOR QUALITY**
- OTHER:** _____

IMAGES ARE BEST AVAILABLE COPY.

As rescanning these documents will not correct the image problems checked, please do not report these problems to the IFW Image Problem Mailbox.